Computer Simulations of Electrokinetic Mass Transport in Microfabricated Fluidic Devices

Sergey V. Ermakov, Stephen C. Jacobson, J. Michael Ramsey

Oak Ridge National Laboratory, P.O. Box 2008, Oak Ridge, TN, 37831-6142, ermakovs@ornl.gov

ABSTRACT

A mathematical model and computer code for simulating electrokinetic fluid and sample manipulations in microfabricated fluidic devices (microchips) are described. The model accounts for mass transport mechanisms such as electrophoretic migration, bulk fluid motion due to electroosmosis, and diffusion. The interactive computer program implementing the model is capable of handling different channel geometries with various boundary conditions for the electric field distribution and sample concentration. Several microchip elements have been modeled and particular attention has been paid to the electrokinetic injection, one of the primary elements in microchip operation. The results obtained in the modeling have been compared with experimental data.

Keywords: Microchip, electrophoresis, electroosmosis, injection.

INTRODUCTION

Over the last five years, microfabricated fluidic devices coupling sample processing and chemical reactions to chemical separations have brought promising results[1-7]. The initial idea of performing rapid electrophoretic separations on the microchip quickly evolved into the concept known as a Lab-on-a-Chip. The microchip is a more complex sample processing unit than conventional HPLC or HPCE units with much broader capabilities. Microchips allow active manipulation of fluids and samples inside a microfabricated channel network as a part of its operating cycle rather than just simple elution afforded by electrophoretic transport and retention. Such fluidic manipulations are based on electrokinetic transport of material exploiting the phenomena of electrophoresis and electroosmosis. Electrophoresis is a motion of electrically charged particles in a medium, while electroosmosis (electroendoosmosis) involves bulk fluid transport. Electroosmosis originates from the liquid-solid interface due to ionization of the solid surface and through viscous forces, generates bulk fluid motion. Electrokinetic manipulations enable the sample to be delivered to points where it may be chemically modified[5, 8], diluted or mixed with other substances[6,9,10], separated[1-7], and perhaps used for further analysis by coupling the microchip with another analytical technique such as mass spectroscopy[11]. As the Lab-on-a-Chip technology addresses more complex analysis problems, more complex fluidic designs and electrokinetic control strategies are required. At this point computer aided design and analysis tools for prototyping and refining fluidic layouts become necessary. Such tools are expected to reduce the time and the cost for development of microchip devices. This paper describes our efforts in developing such design tools for electrokinetically-driven ionic and fluidic transport on microchip devices.

MATHEMATICAL MODEL

Our primary interest in computer modeling is to be able to simulate the temporal sample evolution inside the channel manifold. Sample mass transport in electrophoresis is the result of three major mass transport mechanisms: convection, electrophoretic transport, and diffusion. Bulk convective flow of liquid arises from one or a combination of the following factors: (i) a pressure difference applied to the separation column ends, (ii) electroosmotic flow which has its origin at the column walls, and (iii) thermal convection due to Joule heating. Electrophoretic transport is determined by the electric field distribution which depends upon the boundary conditions and the conductivity of the solution at each point along the channel, which in turn depends on the chemical composition of the solution. Diffusion takes place whenever a spatial non-uniformity in the composition of the solution exists. These three sample transport mechanisms depend on other physical phenomena accompanying electrophoresis: heat transport in the solution, chemical reactions within the buffer, and, of course, the electric field distribution. Mathematical models of electrophoresis formulated previously[12, 13] take into account all the phenomena mentioned above, but in many situations the contributions of different phenomena to the evolution of the electrophoretic system are not equally important.

The nature of experiments and the range of operating conditions used in microchip devices allow us to assume some simplifications in the model which should not substantially effect the accuracy in describing the separation

phenomena[14]. First, we assume the sample concentration to be small compared to the concentration of the buffer solution and the conductivity of the solution to be uniform throughout the liquid volume. At the same time the concentration of the buffer solution is large enough so that the thickness of the electric double layer on the channel walls is negligible compared to the channel dimensions. As a consequence, the convective boundary layer will be of the same order of magnitude as the electric double layer and results in the flat electroosmotic flow profile[15]. Second, we assume that Joule heating in the liquid volume is insignificant, and the temperature of the solution is uniform. In addition the other thermophysical parameters such as diffusion coefficients, fluid viscosity, electrokinetic mobilities, and dielectric properties are considered constant. Third, we assume that all channels have constant depth and that physico-chemical properties of the chip substrate and the cover plate are identical and uniform. Under these conditions fluid flow will be essentially two-dimensional and will not depend on the coordinate normal to the chip plate[15]. A typical geometry of the microchip channels is shown on Fig.1.

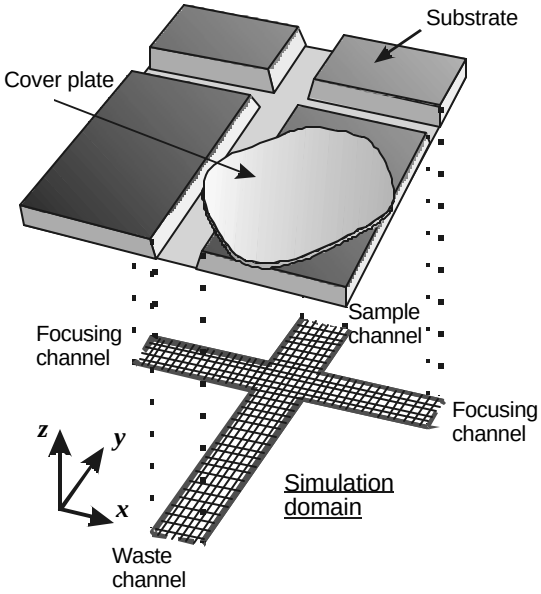

Figure 1. Channel cross geometry used for injection and the corresponding 2-D computational domain.

With the above approximations, the set of equations describing the electric field (eq.1), sample mass transport (eq. 2) and fluid flow (eqs. 3-4) is the following:

$$\nabla^2\Phi = 0, \quad \vec{E} = -\nabla\Phi \tag{1}$$

$$\frac{\partial C_i}{\partial t} + \nabla\left((\vec{V} + \vec{V}_{ep}^{\,i})C_i\right) = D_i\nabla^2 C_i, \quad \vec{V}_{ep}^{\,i} = m_i\vec{E} \tag{2}$$

$$\frac{\partial \vec{V}}{\partial t} + (\vec{V}\nabla)\vec{V} = -\frac{1}{r}\nabla p + n\nabla^2\vec{V}, \tag{3}$$

$$\nabla\cdot\vec{V} = 0, \tag{4}$$

The differential equations (1)-(4) are solved using finite-difference algorithms similar to those described elsewhere [16]. The simulation domain under consideration is covered by a rectangular grid (Fig. 1). The computational algorithm used for solving the Navier-Stokes equations was the following:

$$\frac{\tilde{V} - V^n}{t} + (V^n\nabla)\tilde{V} = -\frac{1}{r}\nabla p^n + n\nabla^2\tilde{V} \tag{5}$$

$$\nabla^2(dp) = \frac{\nabla\tilde{V}}{t}, \qquad dp = p^{n+1} - p^n \tag{6}$$

$$\frac{V^{n+1} - \tilde{V}}{t} = -\nabla(dp) \tag{7}$$

where the velocity $\tilde{V}$ is an intermediate value, and dp is the pressure increment in time. The discrete equations (1),(2),(5),(6) result in a set of linear algebraic equations which are solved by the conjugate gradient method with incomplete Cholesky decomposition. The mathematical model and numerical algorithms were implemented in an in-house written computer simulation program running on Windows-95/NT platform. The program allows to draw interactively the computational domain, specify initial and boundary conditions for the sample concentration and boundary conditions for the electric field (Fig. 2).

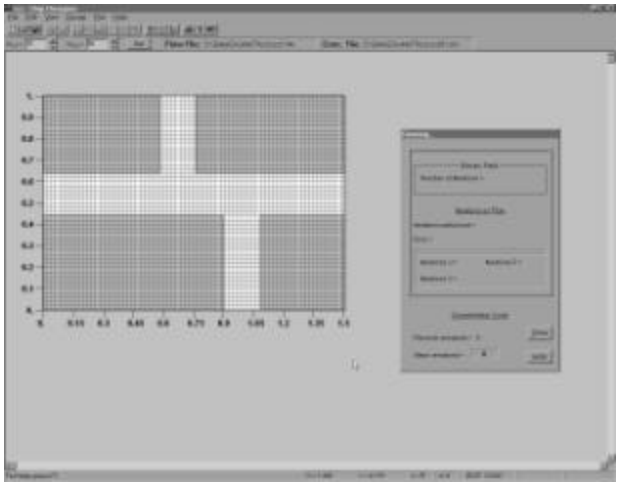

Figure 2. Simulation program (main window). An offset T-injector is depicted.

The output data from the simulation are the spatially dependent velocity, pressure, concentration, and potential fields. Other characteristics including analyte mass, dispersion, and flow rate are then calculated from the output data.

RESULTS

We simulated the operation of the cross intersection (Fig.1) which often used as an electrokinetic valve for sample injection into the separation channel. Two injection

techniques have been demonstrated for the cross valve, pinched injection and gated injection[2]. In the first technique a focusing step precedes the injection step. During focusing the sample flow out of the sample channel is confined by two incoming buffer streams from the side (focusing) channels (Fig. 1) and by the electric field in case of charged particles. The extent of focusing is regulated by the field strength applied to the focusing channels. Once the sample flow has reached a steady state, the field is switched to the injection step when the sample plug is displaced from the injection cross to one of the side channels. Figure 3 shows the focusing step images. The left one is an experimental image giving the laser induced fluorescence (LIF) for a Rhodamine B sample. The right image is a simulated concentration distribution shown in gray scale and agrees well with the experimental data.

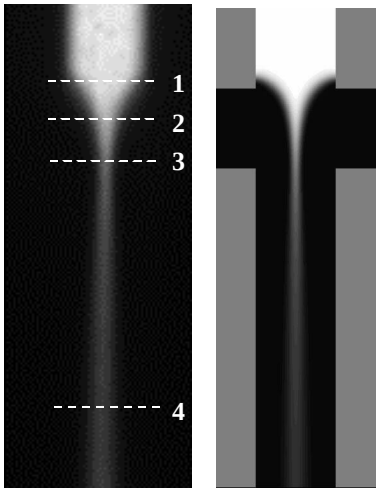

Figure 3. Electrokinetic sample focusing, experimental image (left) and simulated image (right).

A more accurate comparison was performed for the simulated and experimental concentration profiles taking four cross sections at different points along the sample-waste channel (shown by dashed lines on the left panel, Fig. 3). The normalized concentration profiles are shown on Fig. 4. The simulated profiles (solid lines) in panels 2 and 3 are narrower than the experimental ones (dashed lines). In panel 1 the experimental profile gradually approaches zero at the channel edges whereas in the simulation, the concentration on the wall has a value of *ca* 0.4 . Among possible explanations for these discrepancies between experiment and theory are the simplifications adopted in the model, and incomplete experimental data. In the first case we refer to the fact that a 2-D model instead of a 3-D one was considered. The model, therefore, does not account for the actual trapezoidal shape of the channel cross-section (see Fig.1). The LIF signal observed in experiments is integrated over the depth of the channel. Since the channel depth close to the edges is variable (trapezoid shape) the "optical depth", i.e., the thickness of layer emitting the light, is also variable. Therefore close to the channel edges the intensity of

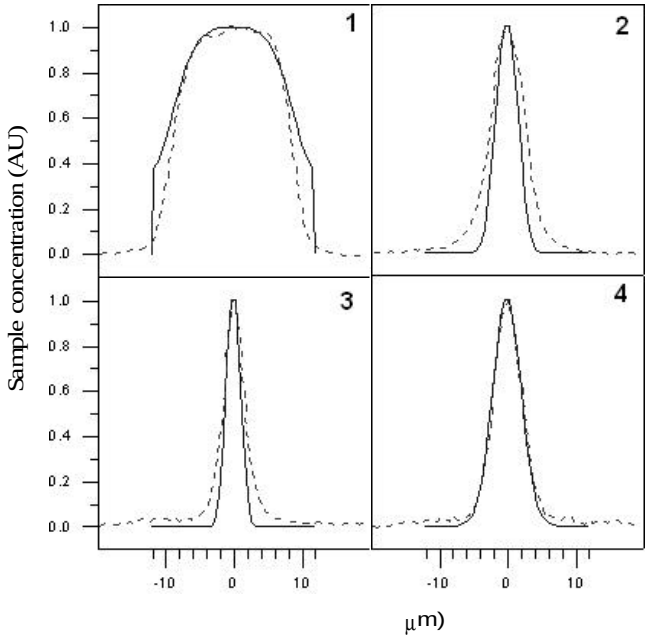

Figure 4. Simulated (solid line) and experimental (dashed line) concentration profiles across the sample waste channel.

light gradually diminishes, giving the impression that the sample stream is smeared. This can probably explain the observed results in Fig.3 (left panel). In addition, as the channel width changes with depth the focusing field may also undergo slight variations along the z-coordinate. The electroosmotic and electrophoretic mobilities were not measured explicitly in these experiments, and therefore, typical values were taken for the simulation.

Figure 5 shows pinched injection sequence when the sample plug initially confined is injected into the separation channel. Two aspects of the pinched valve are important: first, the extent of initial sample confinement, and second, what injection field distribution is optimum. For example, having a narrow sample plug may be very important for some high-speed separations in which initial sample plug width is a key factor in achieving the shortest separation time[17]. Simulations were performed in order to determine optimal running parameters. Thus, during the focusing step there is a compromise between the sample width and its concentration in the injection chamber. Too low of a sample concentration hinders detection. The optimal field scheme for sample loading was found to be: $E_1 = 1$, $E_3 = 0.4$, $E_2 = E_4 = 0.2$, where E_i is the absolute value of the normalized field strength in the *i*-th channel (see Fig. 5). During the injection/separation step it is important to choose the running parameters in such a way that the sample plug will be displaced into channel 4 with minimum axial dispersion and without significant sample losses. A series of simulations revealed that a field distribution when $E_2 = 1$, $E_1 = E_3 = E_4 = 1/3$ was the most suitable for injection/separation.

Figure 5. Pinched injection sequence: focusing step (top), injection (middle), separation (bottom).

REFERENCES

1. Harrison, D. J.; Manz, A.; Fan, Z.; Widmer, H. M. *Anal. Chem.* 1992, *64*, 1926.
2. Jacobson, S. C.; Hergenroder, R.; Kout ny, L. B.; Ramsey, J. M. *Anal. Chem.* 1994, *66*, 1107.
3. Woolley, A. T.; Mathies, R. A. *Anal. Chem.* 1995, *67*, 3676.
4. Jacobson, S. C.; Hergenroder, R.; Koutny, L. B.; Ramsey, J. M. *Anal. Chem.* 1994, *66*, 2369.
5. Jacobson, S. C.; Koutny, L. B.; Hergenroder, R.; Moore, A. W.; Ramsey, J. M. *Anal. Chem.* 1994, *66*, 3472.
6. Hadd, A. G.; Raymond, D. E.; Haliwell, J. W.; Jacobson, S. C.; Ramsey, J. M. *Anal. Chem.* 1997, *69*, 3407.
7. Kutter, J. P.; Jacobson, S. C.; Matsubara, N.; Ramsey, J. M. *Anal. Chem.* 1998, *70*, 3291.
8. Jacobson, S. C.; Hergenroder, R.; Moore, A. W.; Ramsey, J. M. *Anal. Chem.* 1994, *66*, 4127.
9. Harrison, D. J.; Fluri, K.; Seiler, K.; Fan, Z.; Effenhauser, C. S.; Manz, A. *Science* 1993, *261*, 895.
10. Seiler, K.; Fan, Z.; Fluri, K.; Harrison, D. J. *Anal. Chem.* 1994, *66*, 3485.
11. Ramsey, R. S.; Ramsey, J. M. *Anal. Chem.* 1997, *69*, 1174.
12. Babskii, V. G.; Zhukov, M. Y.; Yudovich, V. I. *Mathematical theory of electrophoresis*; Naukova Dimka: Kiev, 1983.
13. Mosher, R. A.; Saville, D. A.; Thormann, W. *The Dynamics of Electrophoresis*; VCH: Weinheim, 1992.
14. Ermakov, S. V.; Jacobson, S. C.; Ramsey, J. M. *Anal. Chem.* 1998, *70*, 4494.
15. Patankar, N. A.; Hu, H. H. *Anal. Chem*. 1998, *70*, 1870.
16. Fletcher, C. A. J. *Computational techniques for fluid dynamics*; Springer-Verlag: Berlin, 1988.
17. Jacobson, S. C.; Culbertson, C. T.; Daler, J. E.; Ramsey, J. M. *Anal. Chem.* 1998, *70*, 3476.